ELSEVIER

Journal of Contaminant Hydrology 51 (2001) 1–12

JOURNAL OF
Contaminant
Hydrology

www.elsevier.com/locate/jconhyd

Field tracer-transport tests in unsaturated fractured tuff

Qinhong Hu *, Rohit Salve, William T. Stringfellow, Joseph S.Y. Wang

Earth Sciences Division, Lawrence Berkeley National Laboratory, University of California, 1 Cyclotron Road, MS 90-1116, Berkeley, CA 94720, USA

Received 6 October 2000; received in revised form 21 March 2001; accepted 21 March 2001

Abstract

This paper presents the results of a field investigation in the unsaturated, fractured welded tuff within the Exploratory Studies Facility (ESF) at Yucca Mountain, NV. This investigation included a series of tests during which tracer-laced water was released into a high-permeability zone within a horizontal injection borehole. The tracer concentration was monitored in the seepage collected in an excavated slot about 1.6 m below the borehole. Results showed significant variability in the hydrologic response of fractures and the matrix. Analyses of the breakthrough curves suggest that flow and transport pathways are dynamic, rather than fixed, and related to liquid-release rates. Under high release rates, fractures acted as the predominant flow pathways, with limited fracture–matrix interaction. Under low release rates, fracture flow was comparatively less dominant, with a noticeable contribution from matrix flow. Observations of tracer concentrations rebounding in seepage water, following an interruption of flow, provided evidence of mass exchange between the fast-flowing fractures and slow- or non-flowing regions. The tests also showed the applicability of fluorinated benzoate tracers in situations where multiple tracers of similar physical properties are warranted. © 2001 Elsevier Science B.V. All rights reserved.

Keywords: Unsaturated zone; Release rate; Fracture–matrix interaction; Flow pathway; Yucca Mountain

1. Introduction

Understanding flow partitioning (i.e., the components of matrix flow, fracture flow, and fracture–matrix interaction) is important for the design and performance of the potential repository at Yucca Mountain. While fast and localized fracture flow has

* Corresponding author. Fax: +1-510-486-5686.
E-mail address: q_hu@lbl.gov (Q. Hu).

0169-7722/01/$ - see front matter © 2001 Elsevier Science B.V. All rights reserved.
PII: S0169-7722(01)00124-3

recently received significant recognition (e.g., Pruess, 1998), the importance of fracture–matrix interaction and matrix flow in delaying contaminant migration should not be overlooked (e.g., Wang and Narasimhan, 1985). Indeed, the relative importance of each flow component is related to numerous factors, which include fracture properties (e.g., length, orientation, aperture, density, and connectivity), matrix properties (e.g., saturation, permeability, and pore-size distribution), and experimental conditions (e.g., test rate, boundary conditions).

McLaren et al. (2000) has recently used a dual continuum model for simulating transient flow and transport at Yucca Mountain. An extensive set of simulations involving a cross-section having properties typical of the site was carried out as a sensitivity study of mechanisms needed to induce fast flow in fractures. Their results indicate that rapid movement of solute through the fractures will not occur unless there are intense episodic infiltration events. Furthermore, field observation that bomb-pulse ^{36}Cl occurs at the repository depth can only be explained if the fracture–matrix coupling term is significantly reduced from a value that would be calculated on the basis of data currently available. They conclude that reliable long-term prediction of repository performance will require extensive subsurface characterization at scales ranging from that of individual fractures to that of regional hydrostratigraphic layers.

This paper presents the results from a field investigation of tracer transport in the welded Topopah Spring unit, the potential repository horizon, at Yucca Mountain. The objective of this effort was to investigate flow and transport behavior under various release rates in the unsaturated fractured rock, using multiple tracers. We hypothesized that flow partitioning and flow pathways are dynamic and related to the experimental release rates. The tests were designed to mimic conditions analogous to transient high-infiltration events.

The use of fluorinated benzoic acids (FBAs) as soil and water tracers has received considerable attention (e.g., Bowman and Gibbens, 1992; Benson and Bowman, 1994; Seaman, 1998). The FBA tracers are attractive because they are generally nonreactive, resistant to degradation, and relatively easy to separate by chromatography and quantify at trace concentrations by UV/Vis spectroscopic detection systems. From the batch test, the FBA tracers are reported to be nonreactive with the tuff at Yucca Mountain over 60 days (Stetzenbach and Farnham, 1996). The choice of 16 derivatives of FBA tracers is also especially useful for studies that require multiple nonreactive tracers. Furthermore, the FBA tracers have larger molecular sizes than the conventional halide tracers, which could be exploited to investigate dispersion in systems where solute transport is affected by the diffusive mass transfer between fast- and slow-flowing regions, such as reported by Hu and Brusseau (1995).

2. Experimental methods

2.1. Tracer tests

Field experiments were conducted in fractured welded tuff within the Exploratory Studies Facility (ESF) at Yucca Mountain. The tuff consists largely ($\sim$ 99 vol.%) of the

former glassy matrix now devitrified to fine crystals of cristobalite, alkali feldspar, and quartz (Johnson et al., 1998). The rock was visibly fractured, with predominantly vertical fractures and a few subhorizontal fractures.

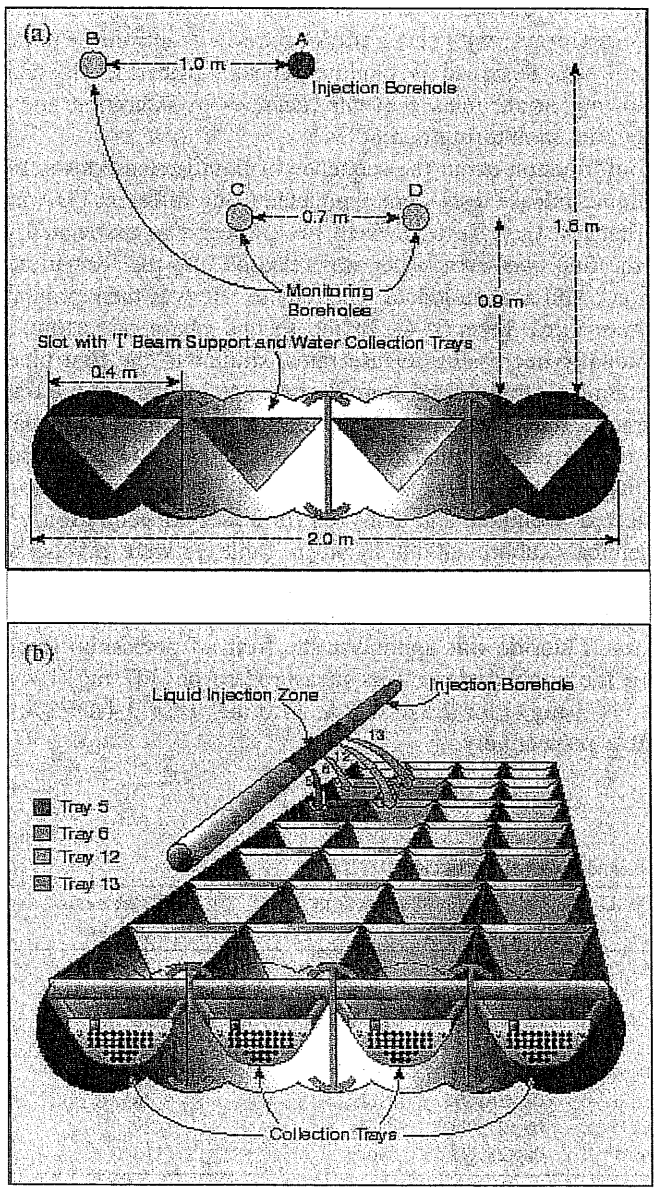

Fig. 1. Schematic showing (a) a vertical view of the test bed layout within the ESF and (b) location of collection trays within the slot; arrows identify trays in which seepage water was collected. Figures are not drawn to scale.

A slot, 2.0-m wide, 4.0-m deep, and 0.3-m high, was excavated by over-coring with a 0.3-m drill-bit to 0.10-m diameter pilot holes drilled. The slot was located about 1.6 m below the injection borehole (Fig. 1a). Liquid injection tests included multiple releases of tracer-laced water in a high-permeability zone (2.3–2.6 m from the borehole collar) within the injection borehole. This zone was delineated from air-permeability measurements conducted before the liquid tests. A water-collection system, consisting of four rows of stainless steel trays, with seven trays each row (each tray with a collection area of 0.46×0.44 m) was designed to capture seepage from the slot ceiling (Fig. 1b). During and following liquid release events, changes in saturation and water potential were monitored in the monitoring boreholes.

Table 1 lists information about the sequence of liquid-release tests. In the first phase of testing, four liquid-release tests were conducted using different FBA tracers as well as fluoride in the first test (i.e., Test 1). Each FBA tracer was associated with a different release rate. In the first two tests, water was released into the formation at the rate that the rock formation could accommodate. The release rate was then gradually decreased in the subsequent tests (i.e., Tests 3–4). In the second phase of testing, four tests were conducted at gradually decreasing release rates, similar to the first phase. These tests, however, did not employ tracers and were designed to investigate the transport behavior of the applied tracers during flushing. The duration of each test was partly dictated by the availability of the underground testing facility, which was normally inaccessible during the nights and weekends. Liquid samples that seeped into the slot were periodically collected, weighed, and analyzed for tracer concentration.

The FBA chemicals (abbreviations listed in Table 1) were purchased from Aldrich Chemical (Milwaukee, WI). The purity was reported to be 99% for PFBA and 2,3,4,5-TeFBA, and 98% for 3,4-DFBA and 2,3,4-TFBA; they were used without further purification. Fluoride was applied in the form of potassium fluoride. The initial concentration for the applied tracer was measured to be 307 mg/l for fluoride, 16.0 mg/l for PFBA, 14.3 mg/l for 2,3,4-TFBA, 17.0 mg/l for 3,4-DFBA, and 17.1 mg/l for 2,3,4,5-TeFBA, respectively.

Table 1
Tracer test conditions and seepage observations

Test phase	Test ID	Date	Tracer used[a]	Release rate (ml/min)	Travel time (minutes)[b]
Phase 1	Test 1	08/04/98	Fluoride and PFBA	119	5
	Test 2	08/04/98	2,3,4-TFBA	98	3
	Test 3	08/05/98	3,4-DFBA	53	3
	Test 4	08/06/98	2,3,4,5-TeFBA	5	300
Phase 2	Test 5	08/25/98	None	69	3
	Test 6	08/26/98	None	38	7
	Test 7	08/27/98	None	29	7
	Test 8	08/28/98	None	14	68

[a]PFBA: pentafluorobenzoic acid; 2,3,4-TFBA: 2,3,4-trifluorobenzoic acid; 3,4-DFBA: 3,4-difluorobenzoic acid; 2,3,4,5-TeFBA: 2,3,4,5-tetrafluorobenzoic acid.

[b]Travel time is defined as the time required for observation of wetting front reaching the slot ceiling.

The construction water in the ESF was used for all of the field liquid tests, and background levels of tracers were measured from the construction-water samples. The construction water originated from the J-13 well water at Yucca Mountain, and was spiked with about 20 mg/l LiBr. Chemical analysis of the contruction water showed that it contained 59 mg/l sodium, 5.9 mg/l potassium, 6.6 mg/l calcium, 0.50 mg/l magnesium, 43 mg/l silicon, 1.4 mg/l fluoride, 6.8 mg/l chloride, and 13 mg/l sulfate. The measured pH value of the construction water was 8.6 ± 0.2 (average $\pm$ standard deviation) for 14 samples. Callahan et al. (2000) reported a similar chemical analysis of the J-13 well water and a pH value of 7.8–8.1. No change in pH was observed for the solutions of stock tracer and tested collected seepage, with the measured pH varying between 8.3 and 8.6 for a total of 14 samples.

2.2. Batch test of fluoride sorption

Laboratory studies on the adsorption potential of fluoride on crushed tuff were conducted using batch-testing techniques under saturated conditions, in accordance with the ASTM method (D4646-87) (ASTM, 1998). Tuff samples were crushed and passed through a 2-mm sieve. A solution to solid ratio of 4:1 was employed instead of the 20:1 ratio specified in the ASTM method. (This was done because a ratio of 20:1 is unrealistically high when compared to that encountered under in situ conditions.) Two initial fluoride concentrations of 327 and 32.7 mg/l, prepared in the construction water, were used in the test to assess the sorption affinity of fluoride with the crushed tuff.

2.3. Tracer analysis

Separation and quantification of FBAs in seepage samples were achieved using a Waters Alliance High Performance Liquid Chromatography (HPLC) System equipped with a Model 996 photodiode array detector. Separations were achieved using a 150×4.6 mm, 5 um LC-PAH column with a C-18 guard column (Supelco, Bellefonte, PA). The FBA tracers, with the injection volume of 10 μl, were separated at a flow rate of 1 ml/min, with a mobile phase of 35% (v/v) acetonitrile and 65% pH 2.9 phosphate buffer. The phosphate buffer was made of 0.058 M KH_2PO_4 by adjusting the pH using an equal molarity of H_3PO4. The concentration of separated FBAs was quantified at a wavelength of 210 nm. Standard solutions to derive the calibration curves comprised of a mixture of these four FBAs. The detection limit of the method for these FBAs was between 5 and 7 ng.

Aqueous fluoride concentration was measured by the Ion Specific Electrode (Orion Ionplus design, Orion Research, Beverly, MA) with the addition of 2% (v/v) ion strength adjuster, as recommended by the manufacturer.

3. Results and discussion

3.1. Field observations

Flint (1998) reported matrix saturations in 266 core samples of welded tuff obtained from the ESF to be $85 \pm 12\%$ (average $\pm$ standard deviation). Water-potential measure-

ments in the monitoring boreholes made with psychrometers prior to the liquid release experiments suggest that a drying front has penetrated ~ 2.0 m into the rock formation from the face of the test bed, the penetration likely resulting from the ventilation of the ESF. We are not aware of in situ measurements of fracture saturation or water potential; however, fractures are expected to be initially dry because of the strong suction of the rock matrix. Numerical simulations of McLaren et al. (2000), for example, reported that fracture saturations are near residual, while the matrix saturation is 0.9 or greater in the welded tuff.

The release rate and travel time for the eight tests are presented in Table 1. Seepage into the slot was observed during all of the tests. During the tests, water initially appeared on the slot ceiling directly below the injection zone and then dripped into one of the four neighboring trays (i.e., Tray 6, Tray 13, Tray 5, and Tray 12; see Fig. 1b). Water dripped into Tray 6 first and with a considerably larger volume than the three other collecting trays (see the *X*-axis of Figs. 2–5). The remaining 24 trays of the collection system did not collect seepage during the tests.

As expected, the travel time for the wetting front was significantly faster at high release rates (29–119 ml/min) and slower for the two low release rates (5 and 14 ml/min) (see Table 1). The role of fractures and the effect of release rates on transport are examined using the tracer breakthrough curves, as discussed in Sections 3.2 and 3.3.

3.2. Tracer transport in the flowing fractures

During tests with the high release rates (Tests 1 and 2), two FBA tracers were immediately observed in the collected samples. The measured concentration was essentially the same as the injected concentration (the C/C_0 value about 0.90–1.04) in Tray

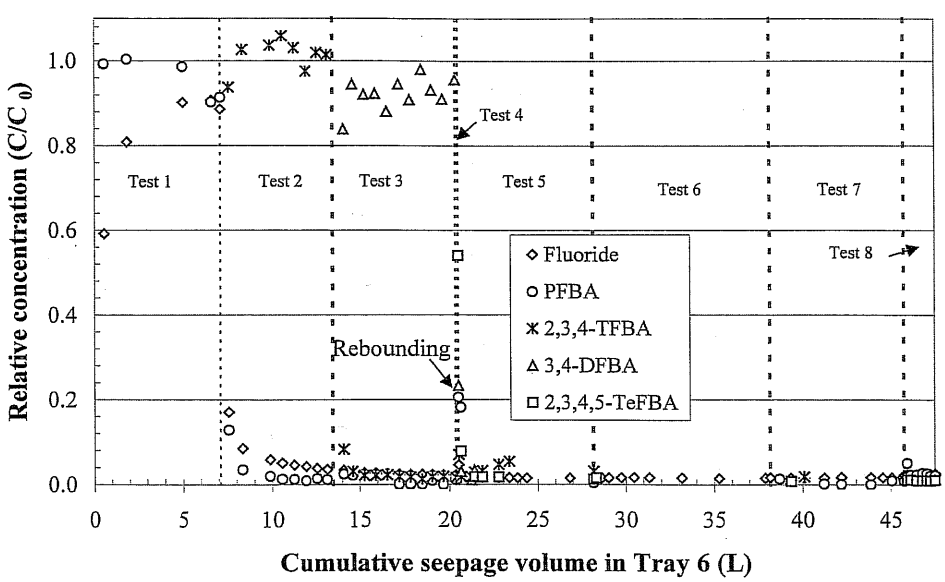

Fig. 2. Measured tracer concentrations versus cumulative seepage volume in Tray 6. Duration of all eight liquid-release tests is identified.

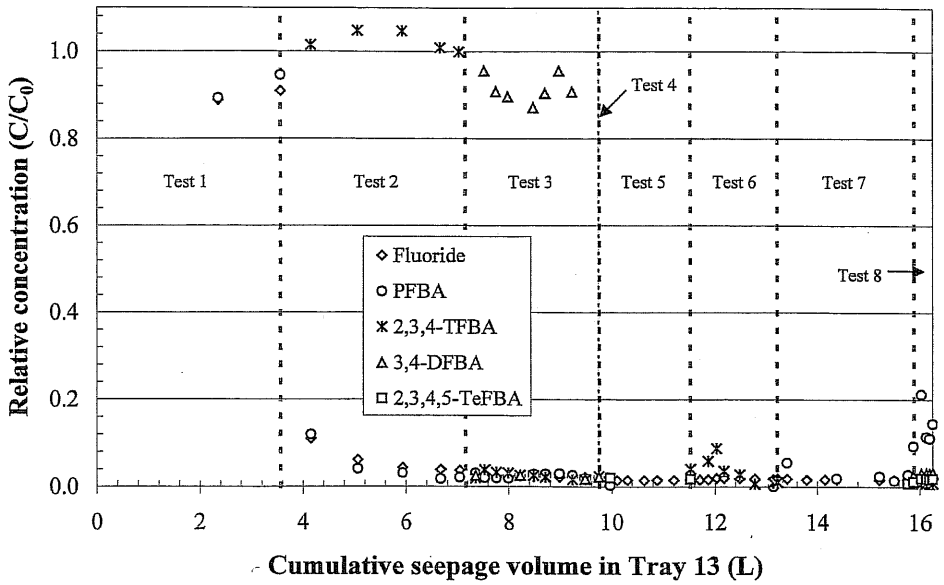

Fig. 3. Measured tracer concentrations versus cumulative seepage volume in Tray 13. Duration of all eight liquid-release tests is identified.

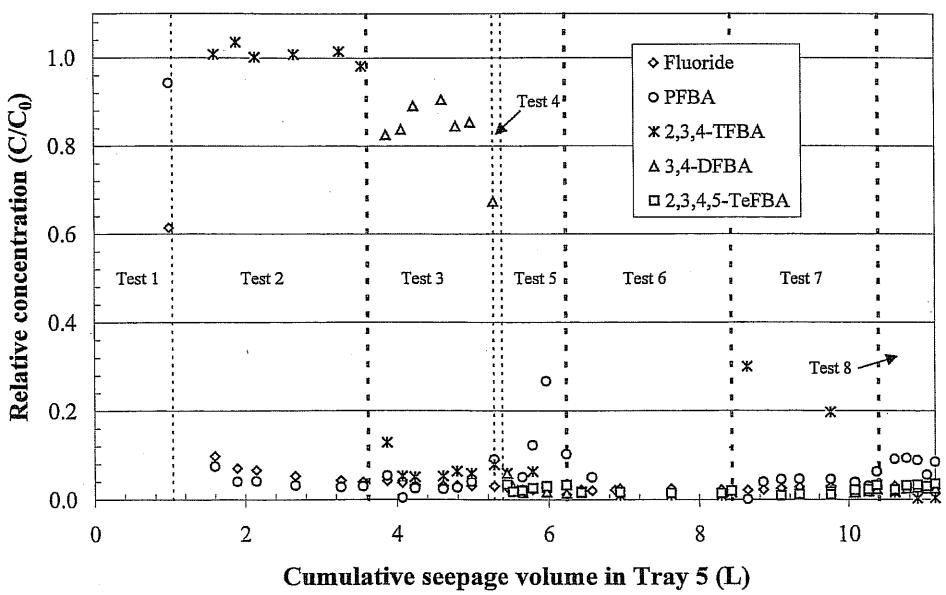

Fig. 4. Measured tracer concentrations versus cumulative seepage volume in Tray 5. All Duration of all eight liquid-release tests is identified.

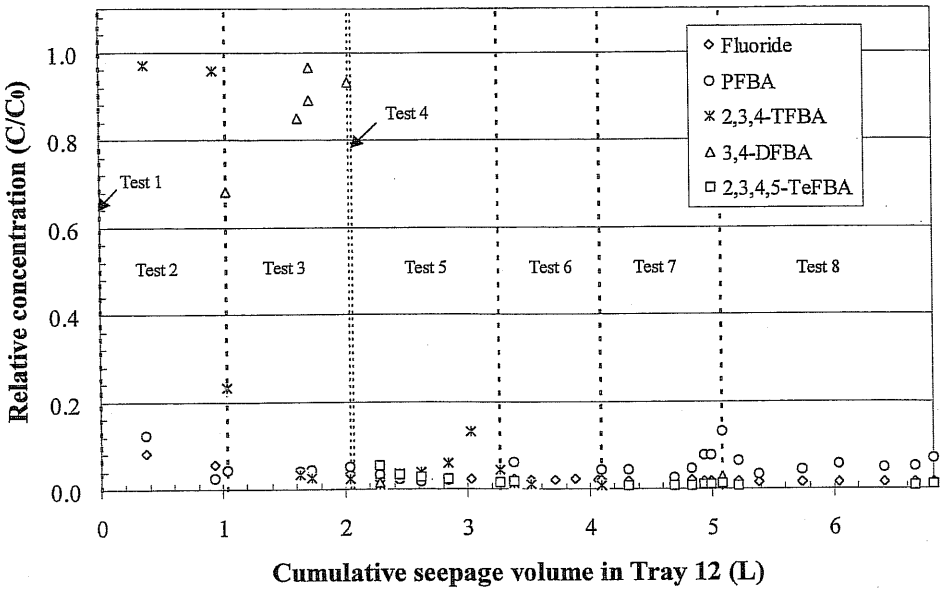

Fig. 5. Measured tracer concentrations versus cumulative seepage volume in Tray 12. Duration of all eight liquid-release tests is identified.

6, Tray 13, and Tray 5 (Figs. 2–4). The travel time in Test 1 over a vertical experimental distance of 1.6 m was about 5 min after only 0.41 l of liquid was released into the formation. The short travel time and high tracer recovery suggest that tracers were transported rapidly through a network of fractures that were connected and flowing. These fractures act as the primary conduits for flow and transport and are likely open-ended throughout the formation.

While there was no seepage in Tray 12 during Test 1, both PFBA and fluoride applied in Test 1 were detected in this tray during Test 2 (Fig. 5). It is likely that some other fractures (which may be small or closed-ended) and matrix flow are responsible for the flow and transport that lead to the seepage and tracer detection in this tray. During Test 1, these flow pathways were either not significantly initiated or not connected with the network of flowing fractures. Once these pathways are activated, they can play an important role, as evidenced from the high C/C_0 values measured for 2,3,4-TFBA applied in Test 2 in Tray 12 (Fig. 5).

3.3. Transport pathways as a function of release rate

As discussed above, tracer transport was dominated by fracture flow under the high release rate of Tests 1 and 2. At the lower release rate of Test 3, the measured C/C_0 of 3,4-DFBA in the seepage of all trays was about 0.82–0.95, suggesting that additional/different pathways were activated during this test. Flow and transport in the lower release rate was likely experiencing a larger portion of the rock formation and therefore was subject to more heterogeneity, as indicated from the enhanced dispersion

(i.e., delay in approaching C/C_0 of 1) in the breakthrough curve for 3,4-DFBA. These additional pathways possibly included the small fractures and, to a certain extent, matrix contributions.

Under the even lower release rate of Test 4, only a total of 0.3 l of seepage was collected from four trays (with the most from Tray 6) out of the total injected volume of 3.4 l. The measured C/C_0 value for 2,3,4,5-TeFBA in the seepage, from the available sample collected from Tray 6, was as low as 0.55. This indicates that more additional pathways were activated under the lower release rate of Test 4. The additional flow pathways could include an important contribution from the matrix flow. This possibility is corroborated by the observation that the wetting front was not observed in the slot ceiling until 1.5 l of liquid was released, as compared to 0.14 l in Test 3. The travel time for the wetting front to reach the slot ceiling was as long as 300 min at the release rate of 5 ml/min for Test 4, compared to 3 min at the release rate of 53 ml/min for Test 3. This much longer travel time, which is not in direct proportion to the release rate, signifies a very important contribution from matrix flow. Nevertheless, it is believed that fracture flow still plays a significant role in controlling tracer transport, as matrix flow alone will not lead to the observed seepage during the experiment duration.

The tracer 2,3,4,5-TeFBA applied at Test 4 resided in the matrix pores and was subsequently flushed and detected in the seepage collected from the four trays during the ensuing flushing tests (Figs. 2–5). The presence of this tracer was even more noticeable in the seepage of Test 8, which had a similar release rate as in Test 4. This indicates that tracer transport in these two tests was likely experiencing similar flow pathways. Seepage from Test 8 also had a high PFBA concentration in Tray 13 and Tray 5 (Figs. 3 and 4), which will be further discussed in Section 3.5 below.

3.4. Transport of fluoride and PFBA

The breakthrough data for Tray 5 and Tray 6 show some differences between PFBA and fluoride, simultaneously injected in Test 1. The measured concentrations of fluoride are lower than that of PFBA, which indicate larger sorption of fluoride in the flow pathways. Fluoride is much more subject to specific chemical binding to mineral surfaces (e.g., Bower and Hatcher, 1967; Kau et al., 1997) than are the FBAs. Stetzenbach and Farnham (1996) reported, from batch and column experiments, that 14 FBA derivatives tested (including the four used in this study) behave conservatively in the tuff of Yucca Mountain.

Our laboratory sorption test confirmed the sorption of fluoride with the crushed tuff, with the measured distribution ratio (ASTM 4646-87) of 1.10 and 4.49 ml/g for the initial fluoride concentration of 32.7 and 327 mg/l, respectively. Note that concerns exist regarding the applicability of the laboratory-derived sorption potential (using crushed-tuff samples and large water/rock ratio under well-mixed condition) to that of the in situ conditions (i.e., large-sized tuff matrix, low water/rock ratio, fast fracture flow). Nevertheless, delayed fluoride transport can be caused from its sorption onto tuff matrix, assisted from the fracture–matrix interaction (discussed in Section 3.5).

Fluoride may also be sorbed onto the fracture-coating minerals. Sorption of fluoride by minerals such as hydrous iron oxide and montmorillonite has been reported by Farrah and Picking (1986) and Bar-Yosef et al. (1988). Triay et al. (1997) listed various

minerals, including manganese and iron oxides/hydroxides, clays, zeolites, and silica, that were found to coat the fracture walls at Yucca Mountain. These fracture-coating minerals are likely present in the rock formation we are testing, and we speculate that they could be responsible for the observed fluoride sorption. Laboratory sorption experiments showed that trace minerals might be quite effective at retarding ^{237}Np (neptunium) transport when they are concentrated on fracture surfaces (Triay et al., 1997). The measured relative concentrations for fluoride and PFBA in Tray 13 (Fig. 3) are overlapping, which might be related to the absence of minerals coating the flowing fractures leading to Tray 13.

Matrix diffusion might also contribute to the delayed fluoride transport compared to PFBA. Because fluoride has a larger aqueous diffusion coefficient in flowing fractures, it will undergo more diffusive mass transfer into the less- or non-flowing regions, leading to its delayed transport. This is deemed a less likely explanation given that matrix diffusion will not be significantly important under the gravity-driven fracture flow. The short travel time observed in the tests would not provide sufficient time for the matrix diffusion to be important. The potential fracture–matrix interaction is expected to involve matrix imbibition owing to the capillarity gradient, rather than matrix diffusion.

3.5. The effect of fracture–matrix interaction

Even in fracture-dominated flow, fracture–matrix interaction can still play an important role, as evident from the tracer test results. Both fluoride and PFBA applied in Test 1 were detected even after the rock formation had been flushed with a large volume of water that was free of these tracers (Figs. 2–5). In Tray 6, for example, fluoride persisted at above the background level in the collected seepage even after six equivalent volumes of tracer-free water seeped (i.e., about 42 l of cumulative seepage volume during Tests 2–4 versus 7 l of seepage from Test 1, shown in Fig. 2). Such long tailing behavior was also true for PFBA (Fig. 2). The long tailing was also observed, to a lesser extent, for 2,3,4-TFBA that was employed in Test 2 (Fig. 2). The 3,4-DFBA applied in Test 3 was even less detectable in the ensuing flushing tests.

Long tailing of PFBA (especially) and 2,3,4-TFBA is likely caused from stronger fracture–matrix interaction during the first two tests, where the formation was less saturated and the matrix block exhibited stronger capillary suctions. This leads to more tracer mass being taken away from the flowing fractures into the matrix and long tailing being observed from the subsequent tests. After tens of liters of injected volume from the first two tests, the flow pathways achieved a "steady-state" condition, with injected tracers undergoing less fracture–matrix interaction than the earlier tests. This is supported by the comparatively shorter travel time and less volume needed to cover the experimental scale in Tests 2–3. During Test 4, which had a much lower release rate, matrix flow contributes to the tracer transport to an important extent, as discussed in Section 3.3.

3.6. Flow interruption

The second-phase testing started 19 days after the end of the first-phase testing. From Test 5, the "rebounding" effect was observed for PFBA seepage concentration in Tray 5

and Tray 6 (Figs. 2 and 4). Rebounding has been reported in flow interruption experiments and gives a clear indication about the mass exchange that takes place between the different flowing regions (e.g., Brusseau et al., 1997; Cote et al., 2000). Our data indicated that, during the interruption, tracers present in the less- or non-flowing regions diffuse towards the boundary with the predominant flow pathways (i.e., fractures) and are readily flushed upon resuming flow. Observation of PFBA rebounding is consistent with the strong fracture–matrix interaction effect, as discussed in Section 3.5.

Fluoride also showed a small, though noticeable, amount of rebounding in the seepage concentrations (Fig. 2). The difference in rebounding between fluoride and PFBA might be related to the different "retardation" mechanism between them. As discussed above, delayed transport of fluoride in Test 1 might be likely related to chemical sorption onto tuff matrix or minerals coating the fracture walls, while PFBA transport undergoes a physical delay from the fracture–matrix interaction that removes it from the flowing fractures into the matrix.

4. Conclusions

This paper was based on a field investigation involving a series of tracer tests in the unsaturated, fractured welded tuff at Yucca Mountain. Analyses of tracer breakthrough curves from collected seepage in the excavated slot below the injection borehole indicate that the flow component partitioning (i.e., relative contribution of fracture flow, fracture–matrix interaction, and matrix flow) and flow pathways change with respect to the experimental conditions, such as the release rate. The regions experiencing flow and transport are dynamic, with more accessible regions under slower experimental rates. Under high release rates, fractures are the predominant pathways, with fracture flow leading to fast transport and long travel distances. Under relatively low release rates, fracture flow will be comparatively less dominant, with a noticeable contribution from matrix flow. Matrix flow will lead to slow solute transport and close contact of solutes with the rock matrix, and consequently sorption and retardation of sorbing contaminants. Slow release rates and dry rock formations are conducive to strong contribution of matrix flow and fracture–matrix interaction, which help retard the migration of contaminants.

Acknowledgements

This work was supported by the Director, Office of Civilian Radioactive Waste Management, US Department of Energy, through Memorandum Purchase Order EA9013MC5X between TRW Environmental Safety Systems, and the Ernest Orlando Lawrence Berkeley National Laboratory (LBNL). The support is provided to Berkeley Lab through the US Department of Energy Contract No. DE-AC03-76SF00098. The authors like to acknowledge the thoughtful comments from Boris Faybishenko, Jianchun Liu, and Dan Hawkes of LBNL. Constructive comments from the anonymous reviewers are also greatly appreciated.

References

ASTM, 1998. Standard test method for 24-hour batch-type measurement of contaminant sorption by soils and sediments (D4646-87). 1998 Annual Book of ASTM Standards. American Society for Testing and Materials, Philadelphia, PA, pp. 44–47.

Bar-Yosef, B., Afik, I., Rosenberg, R., 1988. Fluoride sorption by montmorillonite and kaolinite. Soil Sci. 145 (3), 194–200.

Benson, C.F., Bowman, R.S., 1994. Tri- and tetra-fluorobenzoates as nonreactive tracers in soil and groundwater. Soil Sci. Soc. Am. J. 58, 1123–1129.

Bower, C.A., Hatcher, J.T., 1967. Adsorption of fluoride by soils and minerals. Soil Sci. 103 (3), 151–154.

Bowman, R.S., Gibbens, J.F., 1992. Difluorobenzoates as nonreactive tracers in soil and groundwater. Ground Water 30, 8–14.

Brusseau, M.L., Hu, Q., Srivastava, R., 1997. Using flow interruption to identify factors causing nonideal contaminant transport. J. Contam. Hydrol. 24 (3/4), 205–219.

Callahan, T.J., Reimus, P.W., Bowman, R.S., Haga, M.J., 2000. Using multiple experimental methods to determine fracture/matrix interactions and dispersion of nonreactive solutes in saturated volcanic tuff. Water Resour. Res. 36 (12), 3547–3558.

Cote, C.M., Bristow, K.L., Ross, P.J., 2000. Increasing the efficiency of solute leaching: impacts of flow interruption with drainage of the "preferential flow paths". J. Contam. Hydrol. 43 (3–4), 191–209.

Farrah, H., Picking, W.F., 1986. Interaction of dilute fluoride solutions with hydrous iron oxides. Aust. J. Soil Res. 24, 201–208.

Flint, L.E., 1998. Characterization of hydrogeologic units using matrix properties, Yucca Mountain, Nevada. Water-Resources Investigations Report 97-4243, U.S. Geological Survey, Denver.

Hu, Q., Brusseau, M.L., 1995. Effect of solute size on transport in structured porous media. Water Resour. Res. 31 (7), 1637–1646.

Johnson, J.W., Knauss, K.G., Glassley, W.E., DeLoach, L.D., Tompson, A.F.B., 1998. Reactive transport modeling of plug-flow reactor experiments: quartz and tuff dissolution at 240°C. J. Hydrol. 209, 81–111.

Kau, P.M.H., Smith, D.W., Binning, P., 1997. Fluoride retention by kaolin clay. J. Contam. Hydrol. 28, 267–288.

McLaren, R.G., Forsyth, P.A., Sudicky, E.A., VanderKwaak, J.E., Schwartz, F.W., Kessler, J.H., 2000. Flow and transport in fractured tuff at Yucca Mountain: numerical experiments on fast preferential flow mechanisms. J. Contam. Hydrol. 43, 211–238.

Pruess, K., 1998. On water seepage and fast preferential flow in heterogeneous, unsaturated rock fractures. J. Contam. Hydrol. 30, 333–362.

Seaman, J.C., 1998. Retardation of fluorobenzoate tracers in highly weathered soil and groundwater systems. Soil Sci. Soc. Am. J. 62, 354–361.

Stetzenbach, K., Farnham, I., 1996. Identification and characterization of conservative organic tracers for use as hydrologic tracers for the Yucca Mountain site characterization study, Final Report, Harry Reid Center for Environmental Studies, University of Nevada-Las Vegas, Las Vegas, NV.

Triay, I.R., Meijer, A., Conca, J.L., Kung, K.S., Rundberg, R.S., Strietelmeier, B.A., Tait, C.D., 1997. Summary and synthesis report on radionuclide retardation for the Yucca Mountain Site Characterization Project Milestone 3784M, Los Alamos National Laboratory, Los Alamos.

Wang, J.S.Y., Narasimhan, T.N., 1985. Hydrologic mechanisms governing fluid flow in a partially saturated, fractured, porous medium. Water Resour. Res. 21, 1861–1874.